

# Accepted Manuscript

The influence of gap size on the development of fracture union with a micro external fixator

Richard Meeson, Mehran Moazen, Anita Sanghani-Keri, Liza Osagie-Clouard, Melanie Coathup, Gordon Blunn



PII: S1751-6161(19)30362-5

DOI: <https://doi.org/10.1016/j.jmbbm.2019.07.015>

Reference: JMBBM 3357

To appear in: *Journal of the Mechanical Behavior of Biomedical Materials*

Received Date: 20 March 2019

Revised Date: 31 May 2019

Accepted Date: 18 July 2019

Please cite this article as: Meeson, R., Moazen, M., Sanghani-Keri, A., Osagie-Clouard, L., Coathup, M., Blunn, G., The influence of gap size on the development of fracture union with a micro external fixator, *Journal of the Mechanical Behavior of Biomedical Materials* (2019), doi: <https://doi.org/10.1016/j.jmbbm.2019.07.015>.

This is a PDF file of an unedited manuscript that has been accepted for publication. As a service to our customers we are providing this early version of the manuscript. The manuscript will undergo copyediting, typesetting, and review of the resulting proof before it is published in its final form. Please note that during the production process errors may be discovered which could affect the content, and all legal disclaimers that apply to the journal pertain.

1   **TITLE: The influence of gap size on the development of fracture union with a micro  
2   external fixator**

3   AUTHORS: Richard Meeson<sup>1,2</sup> Mehran Moazen<sup>1,3</sup>, Anita Sanghani-Keri<sup>1</sup>, Liza Osagie-Clouard<sup>1</sup>,  
4   Melanie Coathup<sup>1,4</sup> Gordon Blunn<sup>1,5</sup>

5   <sup>1</sup>Division of Surgery, University College London, Stanmore, UK; <sup>2</sup>Royal Veterinary College,  
6   Hertfordshire, UK; <sup>3</sup>Mechanical Engineering, University College London, <sup>4</sup>University of Central  
7   Florida, USA; <sup>5</sup>University of Portsmouth, Portsmouth, UK

8

9   Corresponding Author: Richard Meeson, r.meeson@ucl.ac.uk

10   Principal Clinical Research Fellow, Division of Surgery, Institute of Orthopaedics and  
11   Musculoskeletal Science, University College London, Royal National Orthopaedic Hospital,  
12   Stanmore, HA7 4LP

13

14

15

16

17

18

19

20

21

22 **Abstract** (250)

23 Increasingly, the rat femoral fracture model is being used for preclinical investigations of  
24 fracture healing, however, the effect of gap size and its influence on mechanobiology is not  
25 well understood. We aimed to evaluate the influence of osteotomy gap on osteotomy healing  
26 between the previously published extremes of guaranteed union (0.5mm) and non-union  
27 (3mm) using this model.

28 A femoral osteotomy in 12-14 week old female Wistar rats was stabilised with a micro fixator  
29 (titanium blocks, carbon fiber bars) with an osteotomy gap of 1.0mm (n=5), 1.5mm (n=7),  
30 2.0mm (n=6). After five weeks, the left femur was retrieved. The osteotomy gap was scanned  
31 using X-ray microtomography and then histologically evaluated. The radiographic union rate  
32 (complete mineralised bone bridging across the osteotomy) was three times higher for the  
33 1.0mm than the 2.0mm gap. The 1.0mm gap had the largest callus ( $0.069\text{um}^3$ ) and bone  
34 volume ( $0.035\text{um}^3$ ). Callus and bone volume were approximately 50% smaller within the  
35 2.0mm gap.

36 Using cadaveric rat femurs, stabilised with the external fixator, day 0 mechanical assessment  
37 of construct stiffness was calculated on materials testing machine displacement vs load output.  
38 The construct stiffness for the 1.0, 1.5 and 2.0mm gaps was  $32.6 \pm 5.4$ ,  $32.5 \pm 2.4$ , and  $32.4 \pm 8.3$   
39 N/mm ( $p=0.779$ ). Interfragmentary strain (IFS) was calculated using the change in osteotomy  
40 gap displacement as measured using microstrain miniature differential reluctance transducer  
41 spanning the osteotomy gap. Increasing the gap size significantly reduced the  
42 interfragmentary strain (IFS) ( $p=0.013$ ). The mean 'day 0' IFS for the 1.0, 1.5 and 2.0mm  
43 gaps were  $11.2 \pm 1.3$ ,  $8.4 \pm 1.5$  and  $6.1 \pm 1.2\%$  respectively.

44 A 1.5mm gap resulted in a delayed fracture healing by 5 weeks and may represent a useful  
45 test environment for fracture healing therapy. Increasing gap size did not affect construct

46 stiffness, but did reduce the ‘day 0’ IFS, with a doubling of non-union and halving of bone  
47 volume measured between 1.0 and 2.0mm gaps.

48 **KEYWORDS (6)**

49 Interfragmentary strain, Fracture biomechanics, Rodent, Delayed-union, Non-union, Fracture  
50 healing

51 **1.1 Introduction**

52 Pre-clinical experimental studies frequently use delayed or non-union models to evaluate a  
53 therapy (Garcia et al., 2013). These are typically created by either mechanical instability,  
54 damaging the vascular supply or introducing material to prevent bridging (Mills and Simpson,  
55 2012). The most common method is to establish a critical sized defect, which is defined as the  
56 minimum amount of bone loss that will not heal by bone formation during the animals  
57 lifetime (Schmitz and Hollinger, 1986). Historically, studies investigating fracture biology  
58 and mechanics have been dominated by large animal models, typically sheep and goats,  
59 however the use rodent models has significantly increased to nearly 50% of all fracture  
60 studies over the last two decades (Garcia et al., 2013), and the rat is used for around one third  
61 of all in vivo fracture studies (Mills and Simpson, 2012). The size of a ‘critical sized defect’  
62 in rats varies between studies, and reflects in part the differing mechanics of their chosen  
63 stabilisation, and whether periosteal stripping is performed. Typically, researchers have used  
64 defects of up to 8mm and as low as 0.5mm in rat fracture studies (Garcia et al., 2013; Mills  
65 and Simpson, 2012).

66 External fixators are commonly used to stabilise a defect due to their ease of application,  
67 minimal interference with subsequent analysis and their potential to alter the mechanical  
68 environment throughout the experiment. However, the literature on rodent fracture

69 biomechanics using external fixators is limited. The most common fixators in use for rodents  
70 are the thermoplastic polyether ether ketone (PEEK) Glatt fixator from the AO Research  
71 Institute Davos (Glatt and Matthys, 2014), which is commercially available and the titanium  
72 alloy ‘Harrison style’ fixator(Harrison et al., 2003; Ho et al., 2014; Lee et al., 2005; Smitham  
73 et al., 2014). The more rigid Harrison fixator (Osagie-Clouard et al., 2018), is a unilateral  
74 uniplanar fixator with a double carbon fiber connecting bar, which has the novel function of  
75 permitting variable gap size, by sliding the adjustable distal titanium block along the bar. This  
76 approach to varying gap size maintains the pin to osteotomy gap distance irrespective of gap  
77 size, whereas other micro fixators require an ostectomy of the desired gap distance to vary  
78 said gap. Increasing osteotomy size may also influence bone healing by a potential variation  
79 in bone biology along its length (diaphyseal to metaphyseal). The Harrison style fixator has  
80 previously showed consistent union with a 0.5mm gap and consistent non-union with a 3mm  
81 gap with a rat femoral osteotomy after 5 weeks (Harrison et al., 2003) and in female adult  
82 wistar rats (Lee et al., 2005; Smitham et al., 2014). The AO fixator is considerable less stiff  
83 (Osagie-Clouard et al., 2018) and although studies generally use controls, direct comparison  
84 of results on the biology of fracture fixation using different fixators is probably inappropriate  
85 due to the difference in their mechanics and hence differences in healing.

86 Numerous studies have tested their hypotheses using osteotomy gaps in the range of 1-2mm  
87 in rats, however the biomechanics have only been evaluated with FE modeling (Wehner et al.,  
88 2014). Currently, no studies have made a sequential evaluation of intermediary gap sizes  
89 between guaranteed healing, delayed union and non-union, to identify the point at which  
90 delayed union occurs. Inherently, the biomechanics of the fixator, including the fracture  
91 (osteotomy) gap interfragmentary strain (IFS) (Perren, 1979), and overall construct stiffness,  
92 will affect the outcome. In order to understand the findings from one study to another,  
93 evaluation of the fracture biomechanics would be highly informative.

94 Clinical fractures heal more slowly than expected and are termed delayed unions and some  
95 may fail to heal at all and are termed non-unions. Many pre-clinical studies evaluate  
96 interventions in models that go on to successful union, and therefore may not be an  
97 appropriate test scenario. Likewise, the non-union pre-clinical model may be too challenging  
98 to demonstrate efficacy of a new treatment and therefore the delayed union may a useful test  
99 environment in pre-clinical studies.

100 The hypothesis for our study was that a delayed union type healing would be seen in a gap  
101 size midway between the published established union at 0.5mm and non-union at 3mm when  
102 using the Harrison style fixator at 5 weeks (Harrison et al., 2003; Ho et al., 2014; Smitham et  
103 al., 2014). The objectives were to assess the fracture healing with three intervening gap sizes  
104 and to determine the potential variation in initial mechanical environments in terms of  
105 construct stiffness and interfragmentary strain.

106

107 **2.1 Methods**

108

109 *2.1.1 Fixator Design & Application*

110 The Harrison style fixator is a unilateral uniplanar (Type Ia) external fixator with two  
111 transcutaneous intraosseus pins proximal and two pins distal to a surgically created osteotomy.  
112 It has a double connecting bar (2mm diameter carbon-fiber; epoxy resin matrix bars) with two  
113 titanium connecting blocks which can slide axially along the bar, and secured in position  
114 using miniature grub screws, allowing alteration of the osteotomy gap size (Figure 1). This  
115 gives a consistent positioning of the pins in the bone and a consistent distance from the

116 osteotomy, but varies the bar working length (bar length between the two fixator blocks), as  
117 the osteotomy is increased.

118 Female Wistar rats, 12-14 weeks old (230-300g) had the fixator placed on the left  
119 craniolateral femur following a lateral surgical approach (Harrison et al., 2003). Using a  
120 precision jig-guide, four bicortical 1.4mm diameter end-threaded self-tapping stainless steel  
121 pins were placed in predrilled 1.0mm holes in a cranial to caudal orientation. Consistent  
122 proximodistal positioning was based on the distal extent of the greater trochanter. Pins were  
123 exited through separate skin incisions and the custom variable spacing fixator was attached,  
124 using a precision spacer to ensure a fixed distance between the near cortex and connecting  
125 blocks of 9mm. A mid-diaphyseal femoral osteotomy, with no periosteal stripping was made  
126 using a diamond tipped hand-saw, whilst applying sterile saline coolant/lubricant. Rats were  
127 then randomly assigned to have a 1.0mm, 1.5mm or 2.0mm osteotomy gap using an  
128 appropriately sized precision spacer placed between the ends of the osteotomised bone, and  
129 the grub screws were tightened. The biceps femoris was closed over the osteotomy with a  
130 single horizontal mattress suture (1.5M PDS II, Ethicon), and the skin was closed with an  
131 intradermal continuous suture (1.5M monocryl, Ethicon). Analgesia was provided with  
132 subcutaneous administration of buprenorphine 0.05mg/kg prior to surgery, then three times  
133 daily for 48 hours per os, within a sweetened jelly. Activity was unrestricted post surgery for  
134 5 weeks until euthanasia. All procedures were carried out in accordance with the Animals  
135 Scientific Procedures Act 1986, were approved by the University's Animal Welfare Ethical  
136 Review Board and were aligned to the ARRIVE guidelines. Those taking part in any surgical  
137 procedure held UK Home Office licences.

138 *2.1.2 X-ray microtomography (MicroCT) and Radiography*

139 After 5 weeks, the left femur with the fixator in place was retrieved. In order to reduce  
140 microCT beam-hardening artifact generated from the interaction of the X-ray beam and the  
141 metallic implant, a radiolucent PEEK fixator block was connected externally to the fixator  
142 pins after careful removal of the skin with surrounding soft-tissues, and then without  
143 disturbing the fracture callus the titanium block fixator was then removed. Samples were  
144 fixed in 10% buffered formaldehyde for up to three days. The formalin fixed samples were  
145 wrapped in cling-film to prevent dehydration and mounted into a sample holder for microCT  
146 scanning. Samples were scanned using a Bruker Skyscan 1172 micro-tomograph (Bruker,  
147 Belgium), at 60KV, 167uA with a 0.5mm aluminum filter. A rotation step of 0.5 degrees,  
148 without frame averaging, and an image pixel size of 4.89um was used. A single image capture  
149 image was taken with the image intensification ‘scout’ prior to scanning, for 2D radiographic  
150 assessment of the osteotomy union. Radiographic scouts were randomised and blinded to  
151 score healing according to the AO-ASIF recommendations for long bone fractures; united, not  
152 united or uncertain (Müller et al., 1979) as follows: *Ununited* (Figure 2, 2.0mm osteotomy b))  
153 where there was no mineralized tissue bridging between the ends of the osteotomy; *uncertain*  
154 (Figure 2, 1.5mm osteotomy b)) where there was new bone formation, however a radiolucent  
155 line remained between the proximal and distal segments, and *united* (Figure 2, 1.0mm  
156 osteotomy b)) where no gap between bone ends was visible.

157 MicroCT scans were reconstructed using NRecon (Bruker, Belgium) with smoothing=2, ring  
158 artifact reduction=12% and beam hardening artifact=41%. Analysis was performed with  
159 CTAn (Bruker, Belgium). Using the measuring tool, the centre point of the osteotomy was  
160 determined and the transverse slice at that point was selected as the reference slice. The callus  
161 was isolated using a 2D ROI shrink wrap stretching over holes <40 pixels, despeckled <150  
162 voxels and then 3D analysis was performed. In order to make a direct comparison of healing  
163 between the differing gap sizes, the central 60% of the osteotomy gap. i.e. only new bone

164 formation within the osteotomy was analysed for each size, which translated to 120, 180 and  
165 240 slices at 5 $\mu$ m slice thickness, giving 0.6mm, 0.9mm and 1.2mm osteotomy gap analysis  
166 for the 1.0, 1.5 and 2.0mm gap respectively. Where absolute measures were made in  
167 quantitative morphometrics, such as total bone volume (BV), these were divided by the  
168 number of slices contributing the analysis for each gap size, to allow for a direct comparison  
169 of bone formation despite analysing different volumes.

170 *2.1.3 Histology*

171 Following CT imaging, bones were decalcified in a 12.5% solution of  
172 ethylenediaminetetraacetic acid then sequentially dehydrated for 24 hours, followed by de-  
173 fatting with chloroform for 48 hours and embedded into wax, with the fixator pins orthogonal  
174 to the facing surface of the block. Fixator blocks and pins were removed once the wax had set  
175 and a microtome (ThermoFisher Scientific, UK) was used to make 5 $\mu$ m thick slices. The  
176 alignment of the blocks within the microtome was altered as necessary to ensure a central  
177 sagittal slice through the femur. The position of a mid-sagittal section through the fracture gap  
178 was assessed using the fixator pin tract holes. Wax slices were mounted onto positively  
179 charged glass slides (X-tra, Leica biosystems, UK), de-waxed and then hydrated. Samples  
180 were then stained with Haematoxylin (Sigma-Aldrich, UK) nuclear stain for five minutes.  
181 Excess stain was removed by gentle washing with water for five minutes. Slides were  
182 counterstained in 1% Eosin (Sigma-Aldrich, UK) for four minutes and then washed and  
183 dehydrated in increasing concentrations of alcohol. Slides were cleaned in xylene and  
184 mounted under 40mm coverslips using Pertex Mounting Medium (CellPath plc, UK).

185 *2.1.4 Histomorphometric analysis*

186 Slides were observed under a light microscope (KS-300 Zeiss, UK). Histomorphometric  
187 analysis at 2.5x magnification was performed on the most central slice, using a line-intercept

188 method with a grid scaled to the graticule and drawn using PowerPoint (Microsoft, USA).  
189 The grid covered the entire visual field from top to bottom (lateral to medial cortex) and was  
190 centered over the osteotomy; its width was equivalent to the original 1.0, 1.5 or 2.0mm  
191 osteotomy. Grid squares were 160um in both directions and intersections, giving 75, 120 and  
192 165 intersections evaluated for the 1mm, 1.5mm and 2.0mm gaps respectively. Intersections  
193 were then scored as bone, cartilage, fibrous tissue, vascular (red blood cells seen not within  
194 tissue matrix) or void based upon Hematoxylin and Eosin uptake and cell morphology to  
195 provide a percentage tissue formation.

196

197 *2.1.5 Assessment of fixator biomechanics and immediate IFS at day 0*

198 The fixator was placed as per the surgical description on the femora of cadaveric 18-20 week  
199 old Wistar rats (n=4). Femora with the fixator still attached were then disarticulated at the hip  
200 and stifle and stripped of soft-tissue attachments. An orthogonal (lateral to medial orientated)  
201 0.8mm bicortical hole was drilled between the two proximal and two distal fixator pins. A  
202 microminiature differential variable reluctance transducer (DVRT - accuracy 0.001mm) (Lord  
203 MicroStrain, model 6101-0200, Williston, USA) was then inserted and fixed in position using  
204 cyanoacrylate glue, to quantify fracture movement (Figure 1). Femurs were biomechanically  
205 tested using a materials testing machine (Zwick Roell 5T, UK). They were mounted in an  
206 axial loading jig with the femoral condyles centred over the lower mount and the upper mount  
207 was centred over the femoral head to simulate a physiological loading axis of the femur along  
208 its mechanical axis. This set-up effectively tested the entire construct of fixator and bone as a  
209 single unit. Three gap sizes were evaluated per specimen; 1.0mm, 1.5mm and 2.0mm. The  
210 distal fixator connecting block was loosened to allow insertion of the precision titanium  
211 spacer and then tightened again. The space was then checked a second time prior to loading

212 and again between each repeat by ‘offering-up’ the spacer to the gap. Care was taken to  
213 ensure the gap was even across the width of the osteotomy.

214 The peak vertical force for each hind limb in rats is 60% bodyweight at the walk(Clarke,  
215 1995). A maximum weight of 300g for an individual rat was seen in the in vivo study and  
216 therefore peak-walking load was assumed to be 1.8N. A single cycle non-destructive test was  
217 performed, with a preconditioning load of 0.5N, followed with loading to a maximum of 10N  
218 in compression at 5mm/min, sampling rate of 50Hz. The first cycle was disregarded and then  
219 four repeats were performed per gap size, per sample. The sensor (DVRT) output (i.e.  
220 millivoltage changes) was recorded and the difference pre and at peak load was determined.  
221 This was then converted into a displacement according to manufacturers calibration equation.  
222 The pre load and peak load lengths were then used to calculate IFS based on change in length  
223 divided by the original length. Fixator–bone construct stiffness was determined from the load-  
224 displacement graphs obtained from TestXpert software (Zwick, Roell, UK). A linear  
225 regression line ( $r^2$ ) was calculated for the linear portion and  $r^2 >0.99$  was considered  
226 appropriate for the linear elastic region. The gradient (m) was determined based on a  $y=mx+c$   
227 equation and gave the stiffness.

228

#### 229 *2.1.6 Statistical Analysis*

230 Fishers Exact was used to compare the fracture healing outcome. Normality was determined  
231 using a Shapiro Wilk test and non-parametric tests were performed to compare groups using  
232 Kruskal-Wallis (KW), and Mann-Whitney U (MWU) performed with Bonferroni correction  
233 applied (alpha = 0.05 / number of comparisons). Results were expressed as means  $\pm$  standard  
234 deviations. Tests were analysed with SPSS version 24 (IBM, Chicago, USA).

235

236 **3.1 Results**237 *3.1.1 Radiographic and microCT assessment of healing*

238 As the gap size increased there was an increase in the AO classification of ununited and  
239 uncertain fracture classifications and a concomitant decrease in united rates, with the ununited  
240 rate more than doubling (Table 1, Figure 2b), however this was not significantly different  
241 with Fishers Exact comparison. On MicroCT quantitative morphometric analysis, the 1.0mm  
242 gap size had a larger callus volume ( $0.069\pm0.04\text{um}^3$ ) and bone volume per slice  
243 ( $0.035\pm0.02\text{um}^3$ ); than for the 2.0mm gap size ( $0.029\pm0.03$  and  $0.026\pm0.02\text{um}^3$  respectively -  
244 Figure 2a & 3). Tissue surface area per slice, giving an index of callus size, was higher in the  
245 smallest 1.0mm gap ( $0.41\pm0.22\text{um}^2$ ) than the largest 2.0mm ( $0.14\pm0.12\text{um}^2$ ). The measured  
246 trabecular thickness was higher in the smaller 1.0 gap than the larger 1.5mm gap  
247 ( $0.055\pm0.01\text{um}$  and  $0.044\pm0.01\text{um}$ ), however it increased again when the gap size increased  
248 to 2.0mm ( $0.057\pm0.02\text{um}$ ). Full microCT results are summarised in Table 2.

249

250 *3.1.2 Histomorphometric analysis*

251 As gap size increased, the area occupied by bone within the callus decreased, and fibrous  
252 tissue increased (Figure 2c, d). Cartilage tissue was highest in the mid-sized gap, however, the  
253 amount of fibrous tissue was still lower than the biggest gaps. None of these trends were  
254 statistically significant (Table 3 and Figure 4), however clear trends were identified.

255

256 *3.2 Mechanical analysis*

257

258 The mean $\pm$ SD stiffness of the four osteotomised femurs with the fixator in situ for the 1.0, 1.5  
259 and 2.0mm gaps were  $32.6\pm5.4$ ,  $32.5\pm2.4$ , and  $32.4\pm8.3$  N/mm (Figure 5); the gap size over  
260 the ranges tested had no impact on the construct stiffness ( $p=0.779$ ), however gap size did  
261 significantly reduce the IFS in the gap ( $p=0.013$ ), (Figure 6). The mean $\pm$ SD % IFS for the 1.0,  
262 1.5 and 2.0mm gaps were  $11.2\pm1.3$ ,  $8.4\pm1.5$  and  $6.1\pm1.2\%$  respectively.

263 **4.1 Discussion**

264

265 Using the rigid Harrison style micro external fixator, this study demonstrated a predominant  
266 delayed union scenario with an osteotomy gap of 1.5mm after 5 weeks, when compared with  
267 previously published studies using the same fixator and a 0.5mm gap (Harrison et al., 2003;  
268 Smitham et al., 2014). This study also showed a 1mm gap leading to a predominance of  
269 union and the 2mm resulting in a delayed union with an atrophic appearance, indicating non-  
270 union, but our study duration was not of sufficient length for an unequivocal definition.

271 Within each group there was greater variation in healing pattern than shown in the published  
272 0.5mm and 3mm gaps. Most of 2mm fracture gaps had an atrophic style non-union with  
273 medullary capping and a fibrous tissue connection, however it must be considered that a  
274 longer duration study would be required to fulfill current time definitions of delayed union  
275 (Garcia et al., 2013). This study had an end point of 5 weeks to allow comparison to previous  
276 studies that used the same fixator and showed a non-union with a 3mm and union with a  
277 0.5mm osteotomy and the same fixator (Harrison et al., 2003; Ho et al., 2014; Smitham et al.,  
278 2014). Under normal circumstances, rat femoral fracture healing should be achieved by 5  
279 weeks, therefore lack of union indicates delayed or non-union at this stage. Uncertain and un-  
280 united radiographic categories are determined by the radiographic appearance of the fracture

281 are technically both delayed union, as our study is not of sufficient duration to use the term  
282 non-union, and hence it was avoided. A longer study with sequential culling may have given  
283 more information on the rate of healing. This would have allowed us to understand whether  
284 fracture healing is reduced by increasing the gap or totally arrested, however in terms of being  
285 informative for rodent fracture healing studies with typically end points of 5-6 weeks, this  
286 was considered unnecessary, and would have used more animals, contrary to the principles of  
287 the 3Rs.

288 The fixator used in this study has been shown to be significantly stiffer at 4.7 times the axial  
289 stiffness of the commercially available AO fixator (Osagie-Clouard et al., 2018), and hence  
290 will have provided a relatively more rigid fixation. Interestingly, increasing the fracture gap,  
291 which increases the working length of the carbon fiber bars did not have any statistically  
292 significant effect on construct stiffness, indicative of the relatively rigid fixator design  
293 compared with the physiological forces it withstands. Very minor influence on stiffness is  
294 possible, however the group sizes required to determine if extremely small changes were  
295 statistically significant would be prohibitively large. This is useful as it provides an ability to  
296 investigate the influence of gap size in terms of its biological impact and the variation in IFS,  
297 without influencing construct stiffness.

298 The impact of gap size on the healing in this particular model system may be driven by the  
299 biological impact of the gap size on tissue healing, rather than its mechanical effects. Large  
300 animal models have shown that increased fracture gaps with the same IFS had reduced  
301 vascularisation and hence diminished biological ability to heal (Claes et al., 2003). However,  
302 other studies quantifying blood vessel formation have shown no difference between atrophic  
303 non-unions, hypertrophic non-unions and healing fractures (Reed et al., 2002), although  
304 vessels appear at a later stage and therefore early vascularisation may be key (Reed et al.,  
305 2003). The histology in this study also showed a consistent level of vascularisation between

306 different gap sizes and their subsequent healing fates. However, the histologic analysis was  
307 performed at five weeks and therefore it is conceivable with an increasing gap size that the  
308 time required for vascular development could be longer and perhaps critical blood vessel  
309 density it not reached at a sufficiently early time frame.

310

311 Despite the commonplace role of rodents in fracture healing research, most studies have  
312 evaluated the influence of IFS on fracture healing with large animal models *in vivo* (Claes et  
313 al., 2003, 1997; Claes and Heigle, 1999) or using FE model (Comiskey et al., 2010; Steiner  
314 et al., 2014; Wehner et al., 2014). With the increasing use of rodents in bone healing studies,  
315 an understanding of the mechanical environment is needed in rodents. This is the first time  
316 such measures have been directly and accurately measured in an *ex vivo* study in rats, with a  
317 micro-miniature differential variable reluctance transducer (accuracy 0.001mm). The use of a  
318 highly sensitive displacement transducer should give a more accurate measure than those  
319 based on the materials testing machine actuator displacement. However, we acknowledge that  
320 the transducer is measuring displacement in the axis of the transducer and this could vary  
321 across the bone gap itself. Additionally, the exact femoral alignment would also differ *in vivo*,  
322 but approximations are required to test in a material testing machine. The *in vitro* tests to  
323 measure IFS were carried out with the load axially aligned. Due to the orientation of the  
324 femur in the live animal, bending and torsional moments would induce strain. Alignment of  
325 the transducer along a different plane on the femur again may have produced differing results,  
326 however our tests showed that a reduction in IFS was related to an increase in delayed union  
327 indicating that the IFS may be an oversimplification. Critically, the set-up considerations  
328 noted are consistent across the gaps tested, and hence their comparison is still informative.  
329 Future studies could make consideration of multiple gauge assessment to build a composite

330 assessment of interfragmentary motion. It would also be useful to make an ex vivo  
331 comparison this fixator to AO/Glutt fixator for healing over different gap sizes.

332 It should also be noted that the cadaveric femurs were in the 18-20 week range whereas the in  
333 vivo study rats were 12-14 weeks old. This was in part due to a consideration of 3Rs, and  
334 although the physes remain open throughout these ages (Roach et al., 2003), growth is  
335 substantially decelerating, and overall limb length was not expected to change much.  
336 Furthermore, the IFS was calculated using a displacement gauge and fixator which was placed  
337 at a standard distance from the osteotomy irrespective of the overall femoral length, hence  
338 creating a consistent biomechanical environment.

339 In a system where the fixator stiffness is unaffected by increasing gap size, and hence the  
340 change in gap length for a given load is consistent, IFS will arithmetically reduce as the  
341 denominator gap size increases. However, assessment of the initial IFS did not indicate the  
342 subsequent pattern of healing as predicted by Perren's IFS theory of fracture healing (Perren,  
343 1979). IFS theory predicts for a given interfragmentary movement, the bigger the gap, the  
344 lower the IFS, if all other factors remain unchanged. However, large gaps and critical sized  
345 defects, even when fixed very rigidly do not heal, and consistent with these findings, there  
346 was a doubling of ununited fractures and halving of bone volume, with an associated increase  
347 in cartilage in the 1.5mm gap and fibrous tissue within the 2.0mm osteotomy as the gap  
348 increased from 1mm. This corresponded to a 'day 0 equivalent' measure of IFS from 12% to  
349 6% respectively. Overall, the groups with the small gaps and an initial IFS >10% had  
350 improved healing than those with big gaps and an IFS <10%, suggesting gap size biological  
351 factors may overwhelm mechanical factors. Some large animal studies with known gap sizes  
352 and interfragmentary movements have also shown good bone healing with IFS >2-10%  
353 (Claes et al., 1995; Kenwright and Goodship, 1989). Claes et al showed that a high initial IFS,  
354 above the Perren 10% threshold resulted in increased callus formation, however, a larger gap

355 had less bone formation for the same initial strain (Claes et al., 1997). However, although  
356 initial IFS is important in the extreme, when a fracture occurs, an established sequence of  
357 events follows (Elliott et al., 2016), with an initial deposition of strain tolerate tissue, such as  
358 granulation tissue, followed by sequential deposition of more strain intolerant tissues. The  
359 wide tissue cuff or ‘callus’, seen in indirect fracture healing, stiffens the gap, and further  
360 increasing fracture stability and reducing IFS (Perren, 2015). When looking at the bone  
361 surface measures (BS) and tissue surface (TS) measures on microCT, there was a trend for a  
362 smaller callus as the strain reduced, potentially consistent with a bigger callus cuff being  
363 required when there is a higher IFS. Various models have expanded upon the work of Perren.  
364 Carter and Blenman, suggested that it is not only the amount of strain, but the way the strain  
365 is applied, be it in compression, tension, shear, and further that the degree of vascularisation  
366 plays influence (Carter et al., 1988). Their finite element model also accounted for eccentric  
367 callus formation with an asymmetric cartilage deposition, which was noted in some of the  
368 samples in this study. They suggested this was due to varying hydrostatic forces with a more  
369 ‘compressive microenvironment’ producing more cartilage and a ‘tensile’ environment would  
370 have less callus with a more fibrous character. This is consistent with the types of loading  
371 patterns that will be developed within an osteotomy of the rat femur with its eccentric  
372 mechanical axis and the use of a unilateral external fixator. Prendergast suggested a further  
373 iterative model with two biophysical stimuli; fluid velocity and shear strain components,  
374 playing a role in the solid and liquid phases (Prendergast et al., 1997). However, these are all  
375 models and typically approximate *in vivo* findings in their extremes.

376 Other complicating factors such as increasing animal age (STRUBE et al., 2008) or sex  
377 appear to influence fracture healing in some studies, although in a study by Mehta et al (2010)  
378 the large difference in bodyweight between female and male rats was not controlled (Mehta et

379 al., 2010). This study however, had a tightly controlled age range and hence weight, and all  
380 were female Wistar rats.

381 In conclusion, the fixator design evaluated here provides stable construct/fracture stiffness  
382 over a range of fracture gap sizes. Increasing gap size did not affect construct stiffness, but  
383 did reduce the ‘day 0’ IFS from 12 to 6%, with a doubling of the incidence of non-union and  
384 halving of bone volume measured. This is in contrast to the expected outcome based on IFS  
385 theory, but may be due to the biological impact of the gap size over and above the mechanics  
386 in this model system. This is the first study to evaluate and directly compare a range of gap  
387 sizes between guaranteed union and non-union in a rodent femoral fracture model using the  
388 Harrison style fixator, and the 1.5mm osteotomy gap provided a delayed-union at 5 weeks.  
389 This study provides informative that will be informative to researches using Harrison style  
390 fixators for fracture healing studies in rats, and may allow for more precise selection of gap  
391 size for their investigations than the two extremes previously published (Harrison et al., 2003;  
392 Ho et al., 2014; Smitham et al., 2014).

393

394 **Acknowledgments**

395 This work was funded by a Medical Research Council, UK, grant (MR/N002318/1).

396

397 **Tables:**

398

399 Table 1: Global radiographic scoring of fracture healing at 5 weeks based on the A0-ASIF  
400 system.

401

402 Table 2: MicroCT quantitative morphometry indices of bone formation within the 60% of the  
 403 osteotomy gap where TV ( $\text{um}^3$ ) = tissue volume, BV ( $\text{um}^3$ ) = bone volume, TV/BV (%) =  
 404 percentage bone volume, TS ( $\text{um}^2$ ) = tissue surface, BS ( $\text{um}^2$ ) = bone surface, Tb.Th ( $\text{um}$ )  
 405 = trabecular thickness, Tb.Sp ( $\text{um}$ ) = trabecular separation, Tb.N (1/ $\text{um}$ ) = trabecular number.

406

407 Table 3: Quantification of tissue formed within the gap as percentage total tissue from line  
 408 intercept analysis of Hematoxylin and Eosin stained mid sagittal sections.

409

#### 410 **Figure Legends**

411 Figure 1: Ex-vivo femur loaded from femoral head to condyles in a materials testing machine  
 412 with a cranially applied Harrison style fixator. A Lord microdisplacement sensor was applied  
 413 to the lateral surface (1a = lateral view, 1b = caudal view).

414 Figure 2: Representative images from the analysis of healing for each fracture gap size. 1a)  
 415 Shows the central transverse 5um thick slice from the centre of the osteotomy from microCT  
 416 analysis. b) Shows a lateral-medial radiograph centred over the two innermost fixator pins and  
 417 the osteotomy. c) Shows a 1x magnification image of the central sagittal slice, Haematoxylin  
 418 and Eosin stained. d) Shows a 2.5x magnification image of the central region of the femur  
 419 with the histomorphometric grid applied for quantitative morphometry.

420 Figure 3: Boxplot showing (the average per 5um slice) microCT bone volume (BV  $\text{um}^3$ ),  
 421 with the BV reducing sequentially as the gap size increases.

422 Figure 4: Quantitative morphometric data from the central region of the osteotomy, from the  
 423 2.5x magnification Hematoxylin and Eosin stained slides, showing the mean $\pm$ SEM reduction

424 in % bone formation as the gap size increases, with the 1.5mm gap showing a concomitant  
 425 increase in cartilage tissue, but the 2.0mm showing a concomitant increase in fibrous tissue.

426 Figure 5: Line graph showing the mean±SD construct stiffness (N/mm) measured, with no  
 427 significant change as the gap size increased.

428 Figure 6: Boxplot showing the change in day 0 immediate IFS (%) as the gap size increased.

429

## 430 References

- 431 Carter, D.R., Carter, D.R., Wong, M., Wong, M., 1988. Mechanical stresses and  
 432 endochondral ossification in the chondroepiphysis. *J. Orthop. Res.* 6, 148–154.
- 433 Claes, L., Augat, P., Suger, G., Wilke, H.J., 1997. Influence of size and stability of the  
 434 osteotomy gap on the success of fracture healing. *J. Orthop. Res.* 15, 577–584.
- 435 Claes, L., Eckert-H bner, K., Augat, P., 2003. The fracture gap size influences the local  
 436 vascularization and tissue differentiation in callus healing. *Langenbeck's Arch. Surg.*  
 437 388, 316–322.
- 438 Claes, L.E., Heigele, C.A., 1999. Magnitudes of local stress and strain along bony surfaces  
 439 predict the course and type of fracture healing. *J. Biomech.* 32, 255–266.
- 440 Claes, L.E., Wilke, H.J., Augat, P., Rübenacker, S., Margevicius, K.J., 1995. Effect of  
 441 dynamization on gap healing of diaphyseal fractures under external fixation. *Clin.  
 442 Biomech. (Bristol, Avon)* 10, 227–234.
- 443 Clarke, K.A., 1995. Differential fore- and hindpaw force transmission in the walking rat.  
 444 *Physiol. Behav.* 58, 415–419.
- 445 Comiskey, D.P., MacDonald, B.J., McCartney, W.T., Synnott, K., Byrne, J.O., 2010. The role  
 446 of interfragmentary strain on the rate of bone healing—A new interpretation and  
 447 mathematical model. *J. Biomech.* 43, 2830–2834.
- 448 Elliott, D.S., Newman, K.J.H., Forward, D.P., Hahn, D.M., Ollivere, B., Kojima, K., Handley,  
 449 R., Rossiter, N.D., Wixted, J.J., Smith, R.M., Moran, C.G., 2016. A unified theory of  
 450 bone healing and nonunion: BHN theory. *Bone Joint J.* 98-B, 884–891.
- 451 Garcia, P., Histing, T., Holstein, J.H., Klein, M., Laschke, M.W., Matthys, R., Ignatius, A.,  
 452 Wildemann, B., Lienau, J., Peters, A., Willie, B., DUDA, G., Claes, L., Pohlemann, T.,  
 453 Menger, M.D., 2013. Rodent animal models of delayed bone healing and non-union  
 454 formation: a comprehensive review. *Eur. Cell. Mater.* 26, 1–4.
- 455 Glatt, V., Matthys, R., 2014. Adjustable Stiffness, External Fixator for the Rat Femur

- 456 Osteotomy and Segmental Bone Defect Models. *J. Vis. Exp.*
- 457 Harrison, L.J., Cunningham, J.L., Strömberg, L., Goodship, A.E., 2003. Controlled induction  
458 of a pseudarthrosis: a study using a rodent model. *J. Orthop. Trauma* 17, 11–21.
- 459 Ho, C.-Y., Sanghani, A., Hua, J., Coathup Melanie Jean, P., Kalia, P., Blunn, G., 2014.  
460 Mesenchymal stem cells with increased SDF-1 expression enhanced fracture healing.  
461 *Tissue Eng. Part A* 140924064904001.
- 462 Kenwright, J., Goodship, A.E., 1989. Controlled mechanical stimulation in the treatment of  
463 tibial fractures. *Clin. Orthop. Relat. Res.* 36–47.
- 464 Lee, O.K., Lee, O.K., Coathup, M.J., Coathup, M.J., Goodship, A.E., Goodship, A.E., Blunn,  
465 G.W., Blunn, G.W., 2005. Use of mesenchymal stem cells to facilitate bone regeneration  
466 in normal and chemotherapy-treated rats. *Tissue Eng.* 11, 1727–1735.
- 467 Mehta, M., Schell, H., Schwarz, C., Peters, A., Schmidt-Bleek, K., Ellinghaus, A., Bail, H.J.,  
468 Duda, G.N., Lienau, J., 2010. A 5-mm femoral defect in female but not in male rats leads  
469 to a reproducible atrophic non-union. *Arch. Orthop. Trauma Surg.* 131, 121–129.
- 470 Mills, L.A., Simpson, A., 2012. In vivo models of bone repair. *J. Bone Jt. Surgery, Br. Vol.*  
471 94, 865–874.
- 472 Müller, M.E., Allgöwer, M., Schneider, R., Willenegger, H., 1979. No Title, springer.com.  
473 Springer Berlin Heidelberg, Berlin, Heidelberg.
- 474 Osagie-Clouard, L., Kaufmann, J., Blunn, G., Coathup, M., Pendegras, C., Meeson, R.,  
475 Briggs, T., Moazen, M., 2018. Biomechanics of Two External Fixator Devices Used in  
476 Rat Femoral Fractures. *J. Orthop. Res.*
- 477 Perren, S.M., 2015. Fracture healing: fracture healing understood as the result of a fascinating  
478 cascade of physical and biological interactions. Part II. *Acta Chir. Orthop. Traumatol.*  
479 Cech. 82, 13–21.
- 480 Perren, S.M., 1979. Physical and biological aspects of fracture healing with special reference  
481 to internal fixation. *Clin. Orthop. Relat. Res.* 175–196.
- 482 Prendergast, P.J., Huiskes, R., Søballe, K., 1997. ESB Research Award 1996. Biophysical  
483 stimuli on cells during tissue differentiation at implant interfaces. *J. Biomech.* 30, 539–  
484 548.
- 485 Reed, A.A.C., Joyner, C.J., Brownlow, H.C., Simpson, A.H.R.W., 2002. Human atrophic  
486 fracture non-unions are not avascular. *J. Orthop. Res.* 20, 593–599.
- 487 Reed, A.A.C., Joyner, C.J., Isefuku, S., Brownlow, H.C., Simpson, A.H.R.W., 2003.  
488 Vascularity in a new model of atrophic nonunion. *J. bone Jt. Surg. Br. Vol.* 85, 604–610.
- 489 Roach, H.I., Mehta, G., Oreffo, R.O.C., Clarke, N.M.P., Cooper, C., 2003. Temporal analysis  
490 of rat growth plates: Cessation of growth with age despite presence of a physis. *J.*  
491 *Histochem. Cytochem.* 51, 373–383. <https://doi.org/10.1177/002215540305100312>
- 492 Schmitz, J.P., Hollinger, J.O., 1986. The critical size defect as an experimental model for

- 493 craniomandibulofacial nonunions. Clin. Orthop. Relat. Res. 299–308.
- 494 Smitham, P., Crossfield, L., Hughes, G., Goodship, A., Blunn, G., Chenu, C., 2014. Low dose  
495 of propranolol does not affect rat osteotomy healing and callus strength. J. Orthop. Res.  
496 32, 887–893.
- 497 Steiner, M., Claes, L., Ignatius, A., Simon, U., Wehner, T., 2014. Numerical Simulation of  
498 Callus Healing for Optimization of Fracture Fixation Stiffness. PLoS One 9, e101370.
- 499 STRUBE, P., MEHTA, M., PUTZIER, M., MATZIOLIS, G., PERKA, C., DUDA, G., 2008.  
500 A new device to control mechanical environment in bone defect healing in rats. J.  
501 Biomech. 41, 2696–2702.
- 502 Wehner, T., Steiner, M., Ignatius, A., Claes, L., 2014. Prediction of the Time Course of  
503 Callus Stiffness as a Function of Mechanical Parameters in Experimental Rat Fracture  
504 Healing Studies - A Numerical Study. PLoS One 9, e115695.
- 505

Gap Size (mm)	Ununited	Uncertain	United
<b>1.0</b>	1/5 (20%)	1/5 (20%)	3/5 (60%)
<b>1.5</b>	3/7 (43%)	2/7 (29%)	2/7 (29%)
<b>2.0</b>	3/6 (50%)	2/6 (33%)	1/6 (17%)

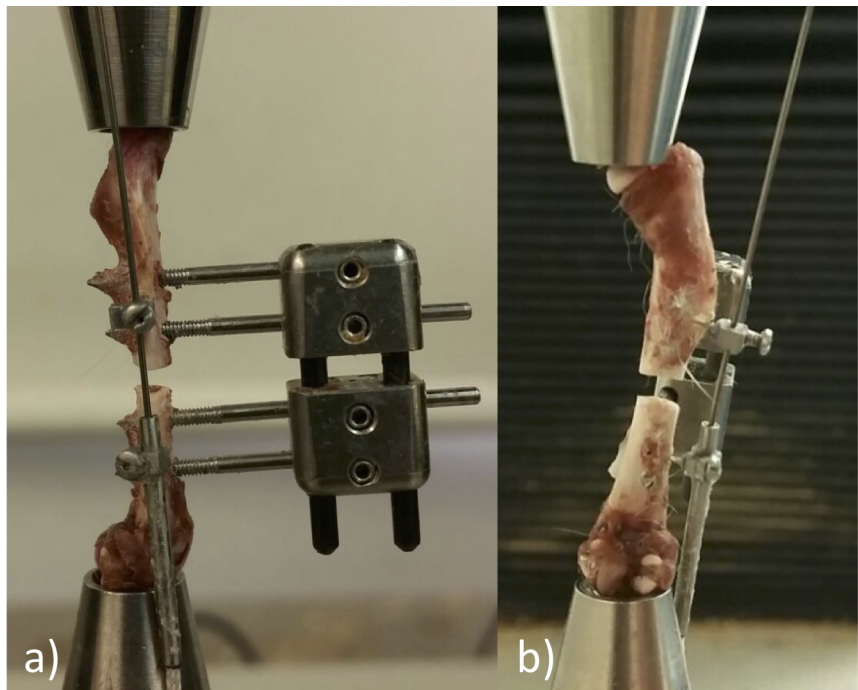
Table 1: Global radiographic scoring of fracture healing at 5 weeks based on the A0-ASIF system.

	<b>1.0mm Gap</b>	<b>1.5mm Gap</b>	<b>2.0mm Gap</b>
<b>TV per slice (<math>\mu\text{m}^3</math>)</b>	0.07±0.04	0.05±0.03	0.03±0.03
<b>BV per slice (<math>\mu\text{m}^3</math>)</b>	0.04±0.02	0.02±0.02	0.02±0.02
<b>BV/TV (%)</b>	54.25±9.38	53.79±20.82	66.39±15.37
<b>TS per slice (<math>\mu\text{m}^2</math>)</b>	0.41±0.23	0.35±0.25	0.14±0.12
<b>BS per slice (<math>\mu\text{m}^2</math>)</b>	2.09±1.62	1.81±1.22	0.90±0.94
<b>Tb.Th (<math>\mu\text{m}</math>)</b>	0.06±0.01	0.04±0.01	0.06±0.02
<b>Tb.Sp (<math>\mu\text{m}</math>)</b>	0.12±0.05	0.07±0.03	0.07±0.05

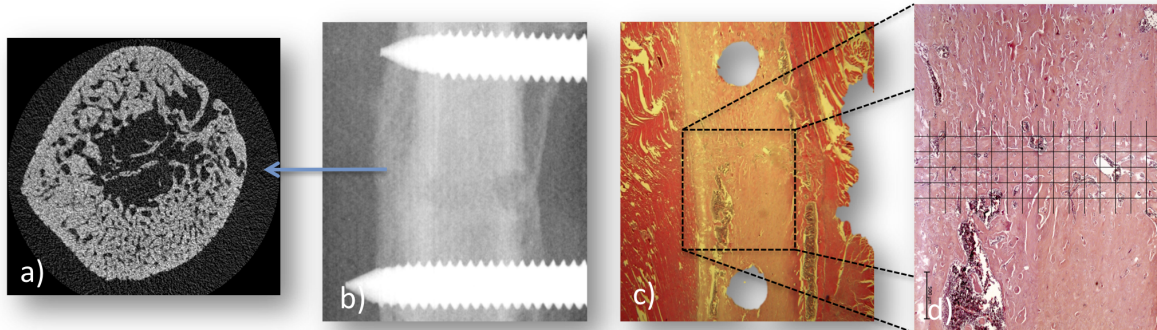
Table 2: MicroCT quantitative morphometry indices of bone formation within the 60% of the osteotomy gap where TV ( $\mu\text{m}^3$ )= tissue volume, BV ( $\mu\text{m}^3$ ) = bone volume, TV/BV (%) = percentage bone volume, TS ( $\mu\text{m}^2$ ) = tissue surface, BS ( $\mu\text{m}^2$ ) = bone surface, Tb.Th ( $\mu\text{m}$ ) = trabecular thickness, Tb.Sp ( $\mu\text{m}$ ) = trabecular separation, Tb.N (1/ $\mu\text{m}$ ) = trabecular number.

% TISSUE	<b>1.0mm Gap</b>	<b>1.5mm Gap</b>	<b>2.0mm Gap</b>
<b>Bone</b>	45.6±33.0	39.1±23.9	23.2±26.6
<b>Cartilage</b>	36.7±22.1	43.1±24.6	37.2±17.9
<b>Fibrous</b>	14.7±30.6	15.3±37.4	36.1±40.8
<b>Vascular</b>	3.0±1.9	2.4±2.0	3.5±3.4

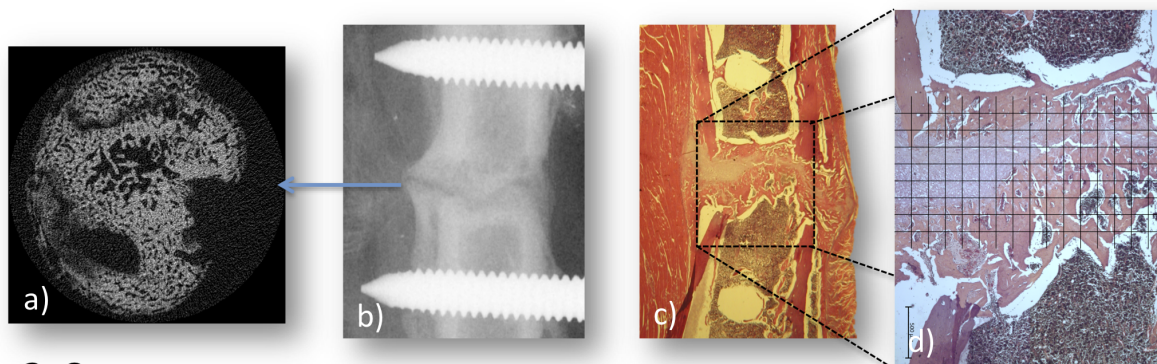
Table 3: Quantification of tissue formed within the gap as percentage total tissue from line intercept analysis of Hematoxylin and Eosin stained mid sagittal sections.



### 1.0mm osteotomy



### 1.5mm osteotomy



### 2.0mm osteotomy

